Arch. Min. Sci. 70 (2025), 3, 377-386
Electronic version (in color) of this paper is available: http://mining.archives.pl

DOI: https://doi.org/10.24425/ams.2025.156290

KRZYSZTOF KRAUZE[1], KAMIL MUCHA[1*],
TOMASZ WYDRO[1], RYSZARD KLEMPKA[2]

MODEL AND ANALYSIS OF ROPE WINCH OPERATION IN UNDERGROUND RAIL TRANSPORT

The primary means of rail transport in inclined workings up to 45° are typically single- or double-drum rope winches. These winches are part of a transport system consisting of the winch itself, a rope with a diameter d and length L_l, a track system, and a return drum with a rope tensioning mechanism. A fundamental challenge in employing winches in a given working is accounting for their operational conditions, which include the route length L_u, its inclination α_u, and the value of the hauled mass (weight) G_m, given a specified load transport velocity v_{pl}. These factors influence the drive load parameters, such as the winding rope force F_C, unwinding rope force F_S, and drive motor power N_p. Manufacturers of these devices provide their structural ($L_{u\,\max}$), kinematic (v_{pj}), and energy-related (N_p) parameters. However, it is the responsibility of the prospective user to assess the suitability of a specific winch for the conditions present in their transport excavation. To address this need, an analytical model, algorithm, and computer program have been developed to dynamically determine the required parameters while considering the winch's operating conditions.

Keywords: Hauling transport; winch-based transport; resistance; drive load; rope elongation; analytical model

1. Introduction

The transportation of various types of machinery, equipment, materials, and personnel can be carried out through haulage (Fig. 1), conveyance (Fig. 2), or hoist (Fig. 3). Haulage refers to a mode of transport that utilizes cars equipped with running gear and wheelsets, moving along different transport routes and powered by various drive systems (electric, hydraulic, internal combustion, or pneumatic) [1,2]. Conveyance is performed using belt, scraper, screw, bucket, plate, or auger conveyors [3,4].

1 FACULTY OF MECHANICAL ENGINEERING AND ROBOTICS, AGH UNIVERSITY OF KRAKOW, AL. MICKIEWICZA 30, 30-059 KRAKOW, POLAND
2 FACULTY OF ELECTRICAL ENGINEERING, AUTOMATICS, COMPUTER SCIENCE AND BIOMEDICAL ENGINEERING, AGH UNIVERSITY OF KRAKOW, AL. MICKIEWICZA 30, 30-059 KRAKOW, POLAND

* Corresponding author: kmucha@agh.edu.pl

Fig. 1. Passenger train in coal mine for miners transportation (haulage) [5]

a) b)

Fig. 2. Belt conveyors transport: a) for people, b) for output [6,7]

Fig. 3. Transport in a shaft under construction (hoisting system) [8,9]

The distinguishing feature of hoisting transport is using a rope or, less commonly, a chain traction system for moving loads. In this system, the transport cars are guided by rail tracks or dedicated guiding structures. Rail transport utilizing winches equipped with ropes falls within this category (Fig. 4) [10,11]. Typically, the movement of valuable loads or personnel in wheel-rail transport cars occurs along transport routes of length L_u, inclined at an angle α_u. A typical transport assembly includes a single- or double-drum winch (1), a rope (2) with a diameter d and length L_l, one or more transport wagons equipped with rail undercarriages (3), a return sheave with a rope tensioning system and rail track (4) (Fig. 5). In inclined workings with a slope of four degrees or more, safety devices (5) are additionally installed to prevent uncontrolled descent of transport wagons in case of rope or winch failure [12,13].

The rope winch is the drive unit within this transport system (Fig. 6) [14]. The rope winch consists of a supporting frame (1), rope drums (2) with a rope (3), planetary gear transmissions (4),

Fig. 4. Transport using rope winch (hauling)

Fig. 5. Transport system with a rope winch in an inclined underground excavation

braking systems, including manoeuvring brakes (5) and a parking brake (6), a drive motor, usually electric or hydraulic. Drum diameter D is selected based on rope diameter d, ensuring compliance with minimum conditions $D \geq 30d$.

The control system for rope winch transport is typically local, though remote operation is also possible in some cases [15]. A prospective user considering rope winch transport is primarily interested in drive parameters, such as load travel speed, maximum rope force and motor power. Determining these parameters requires analytical or empirical evaluation, considering the transport distance and transported mass.

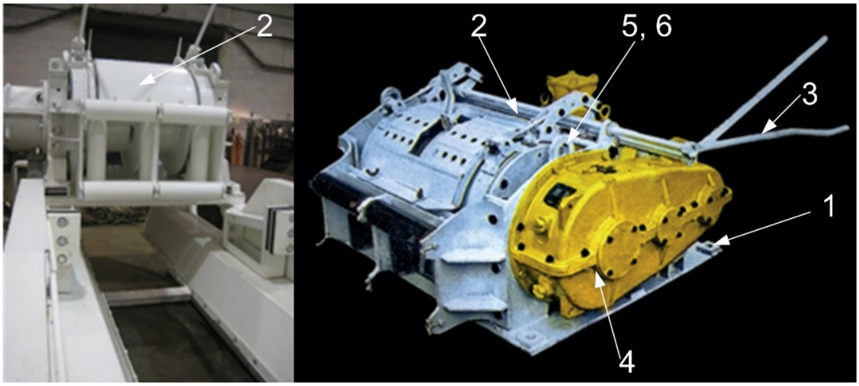

Fig. 6. Double rope drum winch [16,17]

2. Analytical Model of a Transport System with a Rope Winch

As previously mentioned, selecting a suitable rope winch requires determining its technical parameters, preferably through analytical methods. It necessitates the development of an analytical model of a transport system with a rope winch. The schematic diagram of such a transport system operating on an inclined route (working) is presented in Fig. 7. It is assumed that the operation of this transport system is carried out using a winch with an endless rope [15]. The rope wound around the rope drum may be wrapped x times to achieve the required frictional engagement (XP). In an alternative configuration, where the ropes are anchored to the drum, friction between the rope and the drum is not considered.

In the schematic diagram, the individual components of the transport system are designated as follows (Fig. 7):

K_{ZN} – return and tensioning sheave,
K_K – guiding sheave,
C_C – winding rope,
C_S – unwinding rope,
v_{pj} – transport velocity in steady-state motion, m/s,
L_u – length of the transport route (inclined excavation), m,
L_{ul} – distance from arbitrarily selected point A to the guiding sheave K_K, m,

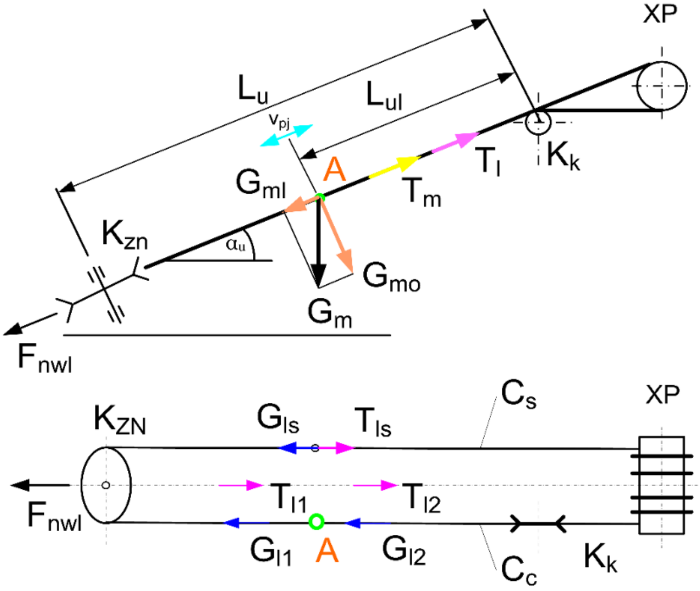

Fig. 7. Schematic diagram of rail transport in an inclined underground excavation using a rope winch (endless rope system)

α_u – inclination angle of the transport route (inclined excavation), °,
q_l – unit weight of the rope, kN/m,
F_{nwl} – initial rope tension force, kN,
G_m – transported weight, kN,
G_{ml} – component of G_m parallel to the floor, kN,
G_{mo} – component of G_m perpendicular to the floor, kN,
G_l – component of the winding rope weight parallel to the floor, kN,
G_{l1} – component of the rope weight section from K_{ZN} to point A parallel to the floor, kN,
G_{l2} – component of the rope weight section from point A to the drive unit parallel to the floor, kN,
G_{ls} – component of the unwinding rope weight parallel to the floor, kN,
μ_{pm} – coefficient of resistance for G_m,
μ_{pl} – coefficient of resistance for the unwinding rope,
μ_{pl1} – coefficient of resistance for the winding rope section from K_{ZN} to point A,
μ_{pl2} – coefficient of resistance for the winding rope section from point A to the drive unit,
T_m – resistance force for the movement of G_m, kN,
T_l – resistance force for the movement of the winding rope, kN,
T_{l1} – resistance force for the movement of the rope section from K_{ZN} to point A, kN,
T_{l2} – resistance force for the movement of the rope section from point A to the drive unit, kN,
T_{ls} – resistance force for the movement of the unwinding rope, kN,
F_C – tension force in the winding rope, kN,
F_S – tension force in the unwinding rope, kN.

Then, using the principle of equilibrium on an inclined plane, the individual forces relevant to selecting the winch, rope, and rope tensioning mechanism were determined.

$$G_{ml} = G_m \cdot \sin\alpha_u \tag{1}$$

$$G_l = G_{l1} + G_{l2} \tag{2}$$

$$G_{l1} = q_l \cdot (L_u - L_{ul}) \cdot \sin\alpha_u \tag{3}$$

$$G_{l2} = q_l \cdot L_{ul} \cdot \sin\alpha_u \tag{4}$$

$$G_{mo} = G_m \cdot \cos\alpha_u \tag{5}$$

$$G_{ls} = q_l \cdot L_u \cdot \sin\alpha_u \tag{6}$$

$$T_m = G_m \cdot \mu_{pm} \cdot \cos\alpha_u \tag{7}$$

$$T_{l1} = q_l \cdot \mu_{pl1} \cdot (L_u - L_{ul}) \cdot \cos\alpha_u \tag{8}$$

$$T_{l2} = q_l \cdot \mu_{pl2} \cdot L_{ul} \cdot \cos\alpha_u \tag{9}$$

$$T_l = T_{l1} + T_{l2} = q_l \cdot \mu_{pl1} \cdot \cos\alpha_u \cdot (L_u - L_{ul}) + q_l \cdot \mu_{pl2} \cdot \cos\alpha_u \cdot L_{ul} \tag{10}$$

$$T_{ls} = q_l \cdot L_u \cdot \mu_{pl} \cdot \cos\alpha_u \tag{11}$$

$$F_s = G_{ls} \pm T_{ls} + 0.5 \cdot F_{nwl} = 0.5 \cdot F_{nwl} + q_l \cdot L_u \cdot (\sin\alpha_u \pm \mu_{pl} \cdot \cos\alpha_u) \tag{12}$$

$$F_C = 0.5 \cdot F_{nwl} + G_{lmC} \pm T_m \pm T_l \tag{13}$$

$$G_{lmC} = G_{ml} + G_l = (G_m + q_l \cdot L_u) \cdot \sin\alpha_u \tag{14}$$

Based on the above dependencies, the values of the individual forces can be calculated, particularly the tension force in the winding rope F_C and the tension force in the unwinding rope F_S, allowing for the selection of the rope diameter d [18,19]. Assuming the required travel velocity v_{pj} for the mass G_m, the motor power of the winch drive N_p can be selected accordingly. The coefficients of resistance μ_{pl1}, μ_{pl2}, and μ_{pl} appearing in these relationships are assumed arbitrarily (empirical values), allowing for two possible cases to be considered. The first case assumes that these coefficients have identical values, leading to:

$$\mu_{pl1} = \mu_{pl2} = \mu_{pl}$$
$$T_l = q_l \cdot \mu_{pl} \cdot L_u \cdot \cos\alpha_u \tag{15}$$

$$F_C = 0.5 \cdot F_{nwl} + (G_m + q_l \cdot L_u) \cdot \sin\alpha_u \pm G_m \cdot \mu_{pm} \cdot \cos\alpha_u \pm q_l \cdot \mu_{pl} \cdot L_u \cdot \cos\alpha_u$$
$$F_C = 0.5 \cdot F_{nwl} + G_m \cdot \sin\alpha_u + q_l \cdot L_u \cdot \sin\alpha_u \pm G_m \cdot \mu_{pm} \cdot \cos\alpha_u \pm q_l \cdot \mu_{pl} \cdot L_u \cdot \cos\alpha_u$$
$$F_C = 0.5 \cdot F_{nwl} + G_m \cdot (\sin\alpha_u \pm \mu_{pm} \cdot \cos\alpha_u) \pm q_l \cdot L_u \cdot (\sin\alpha_u \pm \mu_{pl} \cdot \cos\alpha_u) \tag{16}$$

In the second case, these coefficients have different values, and the lengths of the rope segments before and after point A also differ.

$$\mu_{pl1} \neq \mu_{pl2},\ L_u \geq L_{ul},\ L_{ul} \neq \text{const}$$
$$T_l = q_l \cdot \cos\alpha_u \cdot [\mu_{pl1} \cdot (L_u - L_{ul}) + \mu_{pl2} \cdot L_{ul}] \tag{17}$$

$$F_C = 0.5 \cdot F_{nwl} + (G_m + q_l \cdot L_u) \cdot \sin\alpha_u \pm G_m \cdot \mu_{pm} \cdot \cos\alpha_u \pm$$
$$q_l \cdot \cos\alpha_u \cdot [\mu_{pl1} \cdot (L_u - L_{ul}) + \mu_{pl2} \cdot L_{ul}]$$
$$F_C = 0.5 \cdot F_{nwl} + G_m \cdot (\sin\alpha_u \pm \mu_{pm} \cdot \cos\alpha_u) \pm q_l \cdot L_u \cdot \sin\alpha_u \pm$$
$$q_l \cdot \cos\alpha_u) \cdot [\mu_{pl1} \cdot (L_u - L_{ul}) + \mu_{pl2} \cdot L_{ul}] \tag{18}$$

Using a rope for moving (hoisting) machines, equipment, materials, and people in the case of winches with an endless rope requires the implementation of a rope tensioning mechanism to provide the necessary initial tension force F_{nwl}. The magnitude of this force is determined by the frictional engagement between the rope and the drum and is derived from the force F_C. The force F_{nwl} is typically constant or adjustable, depending on the load conditions.

However, due to the elongation or contraction of the rope under load (resulting from the rheological properties of the rope [20]), its length must be compensated by the rope tensioning mechanism. Therefore, such a mechanism must have an appropriate stroke ΔF_{nwl} and initial rope tension force F_{nwl}. Assuming that ΔF_C represents the elongation of the winding rope under the action of force F_C, and ΔF_S represents the elongation of the unwinding rope under the action of force $F_{S,}$ the unit elongation of the rope q_{lw} can be expressed as:

$$\Delta F_C = q_{lw} \cdot F_C \tag{19}$$

$$\Delta F_S = q_{lw} \cdot F_S \tag{20}$$

Then, the elongation of the rope ΔF_{nwl} under the action of the initial tension force F_{nwl} is determined using equation (22). In contrast, the elongation of the rope under the action of forces F_C and F_S can be obtained from equation (21). The sum of these displacements corresponds to the minimum stroke of the return sheave in the rope tensioning mechanism, as given by equation (23).

$$\Delta F_{CS} = \Delta F_C + \Delta F_S = q_{lw} \cdot (F_C + F_S) \tag{21}$$

$$\Delta F_{nwl} = q_{lw} \cdot F_{nwl} \tag{22}$$

$$\Delta F = \Delta F_{CS} + \Delta F_{nwl} \tag{23}$$

3. Analytical model application

Based on the previously described analytical model and using a spreadsheet, the necessary calculations were performed for a selected transport system with a rope winch installed in an inclined mining excavation of a deep mine (Fig. 8). The purpose of these calculations was to verify the correct selection of the stroke of the return sheave in the rope tensioning mechanism.

The following input data were assumed for the calculations:

- length of the transport route (inclined excavation), L_u = 1150 m;
- distance from arbitrarily selected point A to the guiding sheave K_K, L_{ul} = 500 m;
- unit elongation of the rope q_{lw} = 5.8 mm/kN;
- inclination angle of the transport route (inclined excavation), α_u = 16°;
- transported weight, G_m = 467 kN;
- coefficient of resistance for G_m, μ_{pm} = 0.05;
- required travel velocity, v_{pj} = 2.5 m/s;

Fig. 8. Transport system in the analyzed excavation

- coefficient of resistance for the unwinding rope, $\mu_{pl} = 0.05$;
- coefficient of resistance for the winding rope section from K_{ZN} to point A, $\mu_{pl1} = 0.05$;
- coefficient of resistance for the winding rope section from point A to the drive unit, $\mu_{pl2} = 0.05$.

Initially, a rope with a diameter of $d = 42$ mm ($G_m = 467$ kN) and a unit weight of rope $q_l = 0.08$ kN/m. A preliminary rope pretension force of $F_{nwl} = 20$ kN and a return sheave stroke of $\Delta F = 1000$ mm were adopted. As a result of the calculations (Fig. 9), the tension forces in the winding rope pulling the system upward $F_C = 190.9$ kN and in the unwinding rope $F_S = 30.9$ kN were determined. These results confirm that both the selected rope parameters and the initial rope pretension force are sufficient.

However, the actual return sheave stroke in the rope tensioning mechanism was calculated as $\Delta F = 1143$ mm when moving downward and $\Delta F = 1403$ mm when moving upward. The calculations indicate that the required return sheave stroke exceeds the assumed value by 403 mm, necessitating modifications to the actual system. Of course, similar calculations can be performed with different input parameters to verify whether the theoretical results align with real-world conditions.

5. Conclusions

As previously mentioned, the analytical model of the transport system with a rope winch serves as a support tool in the selection process of the winch and other system components, ensuring suitability for specific operational conditions. Therefore, the future user must be familiar with and capable of defining the requirements for winch, rope, transport route (guidance system), and safety devices. The previously described model is a valuable tool when selecting a rope winch, particularly when determining its technical parameters such as travel speed v_{pj}, transported mass G_m, hauling force F_C, and stroke of the tensioning mechanism ΔF.

Input data for calculations		
Length of the transport route (inclined excavation)	L_u =	1150.00 m
Distance from arbitrarily selected point A to the guiding sheave K_K	L_{ul} =	500.00 m
Inclination angle of the transport route (inclined excavation)	α_u =	16 °
Coefficient of resistance for G_m	μ_{pm} =	0.05
Coefficient of resistance for the winding rope section from K_{ZN} to point A	μ_{pl1} =	0.05
Coefficient of resistance for the winding rope section from point A to the drive unit	μ_{pl2} =	0.05
Coefficient of resistance for the unwinding rope	μ_{pl} =	0.05
Transported weight	G_m =	467.00 kN
Initial rope tension force	F_{nwl} =	20.00 kN
Transport velocity in steady-state motion	v_{pj} =	2.50 m/s
Unit weight of the rope	q_l =	0.08 kN/m
Unit elongation of the rope	q_{lw} =	5.80 mm/kN

Calculations		
Forces and resistances		
Component of G_m parallel to the floor	G_{ml} =	128.72 kN
Component of the rope weight section from K_{ZN} to point A parallel to the floor	G_{l1} =	14.33 kN
Component of the rope weight section from point A to the drive unit parallel to the floor	G_{l2} =	11.03 kN
Component of the winding rope weight parallel to the floor	G_l =	25.36 kN
Component of G_m perpendicular to the floor	G_{mo} =	448.91 kN
Component of the unwinding rope weight parallel to the floor	G_{ls} =	25.36 kN
Resistance force for the movement of G_m	T_m =	22.45 kN
Resistance force for the movement of the rope section from K_{ZN} to point A	T_{l1} =	2.50 kN
Resistance force for the movement of the rope section from point A to the drive unit	T_{l2} =	1.92 kN
Resistance force for the movement of the winding rope	T_l =	4.42 kN
Resistance force for the movement of the unwinding rope	T_{ls} =	4.42 kN
	G_{lmC} =	154.08 kN

Forces in the winding and unwinding ropes during upward and downward movement			
		Downward	Upward
Tension force in the unwinding rope	F_s =	39.78 kN	30.94 kN
Tension force in the winding rope	F_c =	137.21 kN	190.95 kN

Elongation of the winding rope and stroke in the rope tensioning mechanism			
		Downward	Upward
Elongation of the winding rope under the action of force F_C	ΔF_C =	795.84 mm	1107.50 mm
Elongation of the unwinding rope under the action of force F_S	ΔF_S =	230.73 mm	179.43 mm
Total elongation of the rope under the action of forces F_C and F_S	ΔF_{CS} =	1026.57 mm	1286.94 mm
Elongation of the rope under the action of force F_{nwl}	ΔF_{nwl} =	116.00 mm	116.00 mm
Stroke in the rope tensioning mechanism	ΔF =	1142.57 mm	1402.94 mm

Fig. 9. Spreadsheet window for rope winch calculations

References

[1] S. Park, Y. Choi, H. Park, Optimization of truck-loader haulage systems in an underground mine using simulation methods. Geosystem Engineering **19** (5), 222-231 (2016). DOI: https://doi.org/10.1080/12269328.2016.1176538

[2] B. Bharathan, A.P. Sasmito, S.A. Ghoreishi-Madiseh, Analysis of energy consumption and carbon footprint from underground haulage with different power sources in typical Canadian mines. Journal of Cleaner Production **166**, 10, 21-31 (2017). DOI: https://doi.org/10.1016/j.jclepro.2017.07.233

[3] M. Dolipski, P. Cheluszka, F. Remiorz, P. Sobota, Follow-Up Chain Tension in an Armoured Face Conveyor. Archives of Mining Sciences **60**, 1, 25-38 (2015). DOI: https://doi.org/10.1515/amsc-2015-0002

[4] N. Suchorab-Matuszewska, Data-Driven Research on Belt Conveyors Energy Efficiency Classification. Archives of Mining Sciences **69**, 3, 375-389 (2024). DOI: https://doi.org/10.24425/ams.2024.151441

[5] Kopalnia Guido, 2025. Sztolnia: w dawnych wyrobiskach kopalni Królowa Luiza ruszył Karlik i maszyny górnicze https://kopalniaguido.pl/archiwum-wydarzen/1859-sztolnia-dziala-kolejka-karlik-i-nowe-maszyny-gornicze (accessed 21 March 2025).

[6] K. Berezowski, W Halembie pierwsze przenośniki przystosowane do jazdy ludzi pojawiły się już w latach dziewięćdziesiątych. Trybuna Górnicza, 2025. https://nettg.pl/gornictwo/175507/w-halembie-pierwsze-przenosniki-przystosowane-do-jazdy-ludzi-pojawily-sie-juz-w-latach-dziewiecdziesiatych (accessed 21 March 2025).

[7] K. Berezowski, Górnictwo: Przenośniki pod czujnym okiem kamery. Trybuna Górnicza, 2025 https://nettg.pl/gornictwo/172099/gornictwo-przenosniki-pod-czujnym-okiem-kamery (accessed 21 March 2025).

[8] A. Zych, 320 metrów w dół w kuble na urobek. Trybuna Górnicza, 2025. https://nettg.pl/gornictwo/105405/320-metrow-w-dol-w-kuble-na-urobek-galeria (accessed 22 March 2025).

[9] B. Wojsa, Jastrzębska Spółka Węglowa: połączenie szybu 1 Bzie z ruchem Zofiówka. Portal Nasze Miasto, 2025 https://jastrzebiezdroj.naszemiasto.pl/jsw-szyb-1-bzie-polaczony-z-ruchem-zofiowka-foto/ar/c3-3684675 (accessed 22 March 2025).

[10] J.S. Haddad, O. Denyshchenko, D. Kolosov, S. Bartashevskyi, V. Rastsvietaiev, O. Cherniaiev, Reducing Wear of the Mine Ropeways Components Basing Upon the Studies of Their Contact Interaction. Archives of Mining Sciences **66**, 4, 479-594 (2021). DOI: https://doi.org/10.24425/ams.2021.139598

[11] I. Dumitrescu, B.Z. Cozma, V. Itu, Study the mining winches using the CAD/CAE software. International Multidisciplinary Scientific GeoConference: SGEM; Sofia, **2** (2016).

[12] K.A. Yu, T. Yang, Ch.Z. Gong, Design and Research of Double-Drum Winch with Anti-Pressure Wheel. Advanced Materials Research **479-481**, 1709-1713 (2012).
DOI: https://doi.org/10.4028/www.scientific.net/AMR.479-481.1709

[13] M. Sh. Shafi, J. Lu, Z. Song, Y. Fu, Design and tension control of double drum Winch system for deep-sea exploration equipment. Advances in Engineering Research, Proceedings of the 5th International Conference on Information Engineering for Mechanics and Materials 1474-1480 (2015). DOI: https://doi.org/10.2991/icimm-15.2015.269

[14] T.G. Duong, V.T. Nguyen, T.D. Nguyen, Optimizing the weight of the two-level gear train in the personal rescue winch. Archive of Mechanical Engineering **68**, 3, 271-286 (2021). DOI: https://doi.org/10.24425/ame.2021.138393

[15] W. Chen, Sh. Zhu, R. Yue, Design of Control Device for Mine Endless Rope Winch. Advances in Engineering Research, Proceedings of the International Conference on Chemical, Material and Food Engineering, 628-631 (2015). DOI: https://doi.org/10.2991/cmfe-15.2015.149

[16] Vacat Sp. z o.o., 2025. http://www.vacat.pl/oferta/ladowarka-zgarniakowa-vt.html (accessed 26 March 2025).

[17] PPUH "WOJSPOL" Stanisław Wojtala, 2025. https://wojspol.eu/wyroby (accessed 26 March 2025).

[18] L. Kevac, M. Filipovic, A. Rakic, Dynamics of the process of the rope winding (unwinding) on the winch. Applied Mathematical Modelling **48**, 821-843 (2017). DOI: https://doi.org/10.1016/j.apm.2017.02.023

[19] S. Yoo, T. Kim, M. Seo, J. Oh, J. Kim, H. S. Kim, T. W. Seo, Modeling and verification of multi-winding rope winch for facade operation. Mechanism and Machine Theory **155**, 104105 (2021).
DOI: https://doi.org/10.1016/j.mechmachtheory.2020.104105

[20] J.H. Lee, Y.W. Yun, H.W. Hong, et al. Tension control of wire rope in winch spooler using magneto rheological brake. Int. J. Precis. Eng. Manuf. **17**, 157-162 (2016). DOI: https://doi.org/10.1007/s12541-016-0020-1